WETLAND ECOLOGY

High-resolution mapping of losses and gains of Earth's tidal wetlands

Nicholas J. Murray[1]*, Thomas A. Worthington[2], Pete Bunting[3], Stephanie Duce[1], Valerie Hagger[4], Catherine E. Lovelock[4], Richard Lucas[3], Megan I. Saunders[5], Marcus Sheaves[1], Mark Spalding[6], Nathan J. Waltham[1,7], Mitchell B. Lyons[8]

Tidal wetlands are expected to respond dynamically to global environmental change, but the extent to which wetland losses have been offset by gains remains poorly understood. We developed a global analysis of satellite data to simultaneously monitor change in three highly interconnected intertidal ecosystem types—tidal flats, tidal marshes, and mangroves—from 1999 to 2019. Globally, 13,700 square kilometers of tidal wetlands have been lost, but these have been substantially offset by gains of 9700 km^2, leading to a net change of −4000 km^2 over two decades. We found that 27% of these losses and gains were associated with direct human activities such as conversion to agriculture and restoration of lost wetlands. All other changes were attributed to indirect drivers, including the effects of coastal processes and climate change.

Tidal wetlands are of immense importance to humanity, providing benefits such as carbon storage and sequestration, coastal protection, and fisheries enhancement (*1*, *2*). Unfortunately, intensification of anthropogenic pressure and the growing impacts of climate change are affecting tidal wetlands and their component intertidal ecosystems in pervasive ways. Losses of tidal wetlands are widely reported (*3*–*5*), although at local scales intertidal ecosystems are known to have the capacity to respond to environmental change, gaining extent by means of sediment accumulation, inland migration, and redistribution (*6*–*9*). Redistribution and recovery through natural processes are increasingly supplemented by broad-scale ecosystem restoration activities (*10*). Although a number of studies have suggested that intertidal ecosystems are highly resilient to environmental change (*11*, *12*), little is known about the degree to which gains in tidal wetland extent have counterbalanced known losses. Previous analyses have been unable to address this question due to factors such as focus on mapping single ecosystem types (*9*, *13*, *14*) (which cannot distinguish losses from transitions among adjacent intertidal ecosystems), a lack of consistent data on the global extent and change of tidal marshes (*15*), and uncertainty about the prevailing drivers of tidal wetland change. This has led to considerable uncertainty about how tidal wetlands have changed in recent decades and how they are expected to persist in the future (*11*, *12*).

We report an integrated, globally consistent analysis of the distribution and change of Earth's three intertidal ecosystems: tidal flats, tidal marshes, and mangroves (hereafter referred to collectively as "tidal wetlands"; fig. S1). Where they co-occur, these three ecosystems are highly interconnected, with feedback mechanisms among biological and physical components that interact extensively across the systems (*8*). We investigate the spatiotemporal distribution of tidal wetlands globally by applying stacked machine learning classifiers to remotely sensed data to model their occurrence, detect the type and timing of loss and gain events, and assess the drivers of change over the study period (1999 to 2019). The validated dataset was produced by combining observations from 1,166,385 satellite images acquired by the Landsat 5 to 8 missions with environmental data of variables known to influence the distributions of each ecosystem type, including temperature, slope, and elevation (tables S1 and S2). Tidal wetland loss was defined as the replacement of any of the three focal ecosystems with nonintertidal ecosystems at the 30-m pixel scale, with tidal wetland gain defined as their establishment in pixels where they did not occur in 1999. A weighted random sample of detected changes was used to estimate the contribution of direct human impacts versus indirect drivers, such as sea level rise and natural coastal processes, on tidal wetland losses and gains globally (*16*).

Our global dataset reveals that the total observed area of tidal wetlands in 2019 was at least 354,600 km^2 [95% confidence interval (CI): 244,800 to 363,900 km^2]. Tidal wetlands are unevenly distributed across the world's coastlines, with the largest remaining contiguous tracts occurring as deltaic mangroves fringed by extensive tidal flats in the Amazon Delta, the Northern Bay of Bengal, New Guinea, and the Niger Delta (Fig. 1A). Previous estimates of global tidal marsh extent rely on spatial data compilations with large gaps in coverage that lead to underestimates of extent (*15*), limiting their use for estimating global blue carbon stocks (*17*). Our data therefore allow a first empirical estimate of global tidal marsh extent of 90,800 km^2, obtained by subtracting previously derived extent estimates of mangroves (135,900 km^2) and tidal flats (127,900 km^2) from our global tidal wetland area estimate (*9*, *18*). Our estimate of tidal marsh extent represents 25.6% of the total tidal wetland extent mapped in this study and is 65.1% greater than a previously reported minimum global estimate of 55,000 km^2 (*15*). Because our methods are limited in regions higher than 60°N latitude, where tidal marshes and tidal flats are known to occur, this upward revision of global tidal marsh extent should be considered conservative.

We analyzed tidal wetland change over the 20-year study period and found that losses of 13,700 km^2 (95% CI: −16,800 to −8200 km^2) have been substantially offset by the establishment of 9700 km^2 (95% CI: +4900 to +15,700 km^2) of new tidal wetlands that were not present in 1999 (Table 1). Despite wide geographic variation in the occurrence of tidal wetlands globally, many regions showed a consistent pattern of losses being substantially offset by nearby gains (Fig. 1, B and C). This pattern was most pronounced in the world's major river deltas (*19*), where about one-fifth (19.1%) of the area of tidal wetland changes occurred, despite containing only 7.5% of the world's tidal wetland extent (Fig. 2A). We recorded the greatest tidal wetland change in the Ganges-Brahmaputra (1070 km^2) and Amazon deltas (730 km^2), both of which have exhibited increased tidal wetland extent since 1999 (ratio of loss to gain 0.92 and 0.98, respectively). Many deltas have experienced a net increase in total extent over the past three decades as a result of increases in fluvial sediment supply caused by catchment deforestation and increased upland soil erosion (*19*). Our data, however, suggest a net loss of tidal wetlands on deltas globally, though gains of 2100 km^2 alongside losses of −2300 km^2 indicate the considerable dynamism of these systems. The latter have been associated with multiple direct drivers of change, such as conversion to agriculture and aquaculture (*9*, *14*), urban expansion (*20*), and geomorphic changes due to dikes and channel diversions (*20*), together with many indirect drivers, including shoreline erosion (*9*, *20*), compaction, subsidence and sea level rise (*21*), storm-driven

[1]College of Science and Engineering, James Cook University, Townsville, Australia. [2]Conservation Science Group, Department of Zoology, University of Cambridge, Cambridge, UK. [3]Department of Geography and Earth Sciences, Aberystwyth University, Aberystwyth, Wales, UK. [4]School of Biological Sciences, The University of Queensland, Brisbane, Australia. [5]Coasts and Ocean Research Program, CSIRO Oceans and Atmosphere, St. Lucia, Australia. [6]The Nature Conservancy, Department of Physical, Earth, and Environmental Sciences, University of Siena, Siena, Italy. [7]TropWATER, Centre for Tropical Water and Aquatic Ecosystem Research, James Cook University, Townsville, Australia. [8]Centre for Ecosystem Science, School of Biological, Earth and Environmental Sciences, University of New South Wales, Sydney, Australia.
*Corresponding author. Email: nicholas.murray@jcu.edu.au

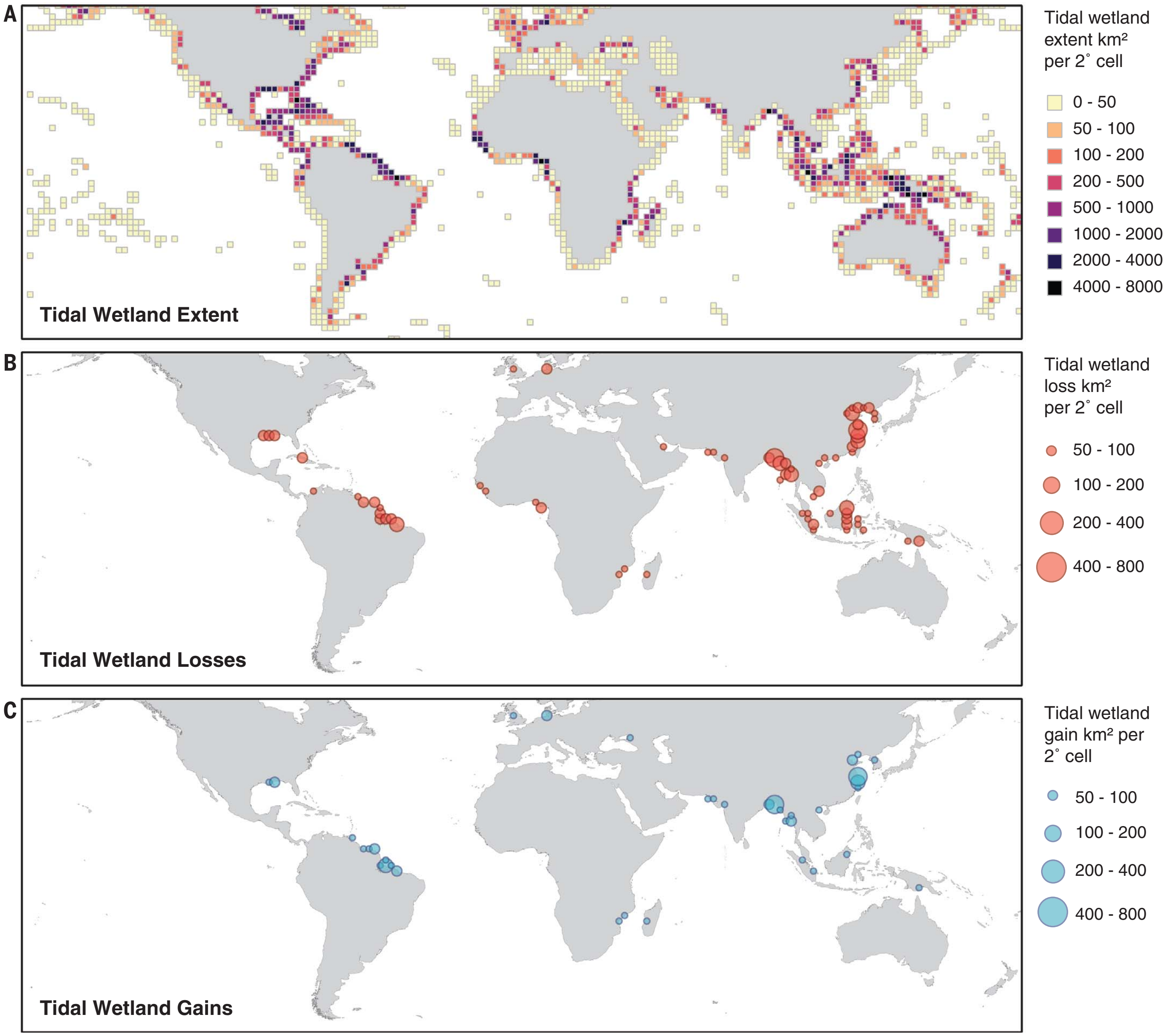

Fig. 1. The global distribution of major tidal wetlands and their changes from 1999 to 2019. (**A**) The 2019 distribution of tidal wetlands is modeled as the combined distribution of the world's three main intertidal ecosystems: tidal flats, tidal marshes, and mangroves. Darker colors indicate greater area of tidal wetlands per 2° grid cell. (**B**) Losses and (**C**) gains over the period 1999 to 2019. Circle sizes indicate the extent of tidal wetland loss and gain over the study period in square kilometers per 2° grid cell.

vegetation loss (*22*), pollution (*23*), and altered sediment supply (*19*).

Of the three intertidal ecosystems included in our analysis, tidal flats experienced both the greatest loss (7000 km^2; 95% CI: 4200 to 8600 km^2) and gain (6700 km^2; 95% CI: 3400 to 10,800 km^2), accounting for almost two-thirds (58.8%) of the total tidal wetland area change (Table 1 and Fig. 3A). A ratio of loss to gain of 1.1 indicates that newly established tidal flats have made a substantial contribution to offsetting the magnitude of their net loss globally. By contrast, mangroves had the highest ratio of loss to gain (3.0), with an estimated net decrease in extent of 3700 km^2 (95% CI: −5400 to −2100 km^2), indicating that extensive mangrove losses have only been partially offset by the 1800-km^2 (95% CI: +900 to +3000 km^2) of new mangroves detected by our analysis. Tidal marshes had the lowest total area change and were the only ecosystem to have a loss to gain ratio of <1, indicating that their gain marginally exceeded their loss for an estimated net increase of 100 km^2 (95% CI: 0 to +100 km^2). Our estimates of global tidal wetland change partitioned by ecosystem type agree in magnitude with recently published estimates of changes in mangrove extent from 2000 to 2016 of −3400 km^2 (*14*). No comparable global estimates of tidal flats and tidal marsh change are available because of differing coverage of change analyses of tidal flats (*9*) and a lack of any data sufficient to support global change analyses of tidal marshes (*15*).

About three-quarters of the 4000 km^2 net global tidal wetland decrease between 1999 and 2019 occurred in Asia (74.1%), with 68.6% concentrated in just three countries: Indonesia

(36%), China (20.6%), and Myanmar (12%). Losses of tropical mangrove forests across Southeastern Asia—particularly Indonesia and Myanmar—are well-documented (*14*, *18*), and the extensive impact of coastal land conversion was confirmed by our analysis (Fig. 3B). In China, there was also a large net reduction of tidal flat extent of >1000 km^2 largely due to reclamation (*24*) but net gains of tidal marshes (+ 200 km^2) that coincided with the rapid expansion of *Spartina alterniflora* across the country's intertidal zone (Fig. 3C) (25), thus reducing China's net tidal wetland loss to 800 km^2 (table S3). Outside of Asia, tidal wetlands in Africa had the highest ratio of loss to gain (1.6), indicating a strong loss dynamic that has been associated with severe mangrove degradation, which is most intense in Nigeria, Mozambique, and Guinea-Bissau (Fig. 1B and table S3).

Interpretation of a globally distributed random sample of tidal wetland losses and gains suggested that 39% of losses and 14% of gains were caused by direct human activities (table S9). Direct human activities were defined as observable activities occurring at the location of the detected change (*26*), including conversion to aquaculture, agriculture, plantations, coastal developments, and construction of physical structures such as seawalls and

Table 1. Tidal wetland change estimates by intertidal ecosystem type for different regions of the world from 1999 to 2019. Change estimates are in square kilometers. Tidal wetlands in this study collectively refer to tidal flat, tidal marsh, and mangrove ecosystems, such that area change of tidal wetlands is the sum of the change area of the three component intertidal ecosystems. Per-pixel losses and gains were summarized at these regional scales, with 95% confidence intervals derived from quantitative accuracy assessment in parentheses. Analysis units are realms from the Marine Ecoregions of the World.

Marine ecoregion realm	Tidal flat		Mangrove		Tidal marsh		Tidal wetlands	
	Loss	Gain	Loss	Gain	Loss	Gain	Loss	Gain
Central Indo-Pacific	−952 (−1169 to −570)	1156 (589 to 1871)	−2719 (−3338 to −1626)	758 (387 to 1227)	−12 (−15 to −7)	7 (4 to 12)	−3683 (−4522 to −2203)	1921 (980 to 3110)
Western Indo-Pacific	−1573 (−1932 to −941)	1741 (888 to 2818)	−1139 (−1398 to −681)	380 (194 to 616)	−18 (−22 to −11)	66 (34 to 107)	−2730 (−3351 to −1633)	2187 (1115 to 3541)
Tropical Atlantic	−1067 (−1309 to −638)	1082 (552 to 1752)	−1541 (−1892 to −922)	567 (289 to 919)	−14 (−18 to −9)	5 (2 to 8)	−2622 (−3219 to −1569)	1654 (844 to 2678)
Temperate Northern Pacific	−2355 (−2891 to −1408)	1415 (722 to 2291)	−31 (−38 to −18)	26 (13 to 43)	−192 (−236 to −115)	428 (218 to 693)	−2578 (−3165 to −1542)	1869 (954 to 3027)
Temperate Northern Atlantic	−594 (−729 to −355)	827 (422 to 1338)	−2 (−2 to −1)	2 (1 to 3)	−680 (−835 to −407)	478 (244 to 774)	−1276 (−1566 to −763)	1307 (667 to 2116)
Tropical Eastern Pacific	−106 (−131 to −64)	110 (56 to 178)	−93 (−115 to −56)	86 (44 to 139)	0 (0 to 0)	0 (0 to 1)	−200 (−246 to −120)	196 (100 to 317)
Temperate South America	−110 (−135 to −66)	117 (60 to 190)	−4 (−5 to −2)	5 (3 to 8)	−66 (−82 to −40)	111 (57 to 180)	−181 (−222 to −108)	233 (119 to 378)
Arctic	−118 (−145 to −71)	173 (88 to 280)	0 (0 to 0)	0 (0 to 0)	−30 (−36 to −18)	36 (19 to 59)	−148 (−182 to −88)	209 (107 to 339)
Temperate Australasia	−86 (−105 to −51)	66 (34 to 107)	−13 (−16 to −8)	2 (1 to 2)	−43 (−53 to −26)	20 (10 to 32)	−141 (−174 to −85)	87 (44 to 141)
Eastern Indo-Pacific	−53 (−65 to −32)	4 (2 to 7)	−1 (−1 to −1)	1 (0 to 1)	0 (0 to 0)	0 (0 to 0)	−54 (−67 to −33)	5 (3 to 8)
Temperate Southern Africa	−9 (−11 to −5)	8 (4 to 13)	−19 (−23 to −11)	1 (0 to 1)	−6 (−7 to −4)	11 (6 to 18)	−33 (−41 to −20)	20 (10 to 32)
Southern Ocean	−4 (−5 to −3)	2 (1 to 4)	0 (0 to 0)	0 (0 to 0)	−1 (−1 to −1)	1 (1 to 2)	−5 (−6 to −3)	4 (2 to 6)
Total	−7028 (−8628 to −4204)	6700 (3418 to 10849)	−5561 (−3326 to −6827)	1828 (932 to 2960)	−1064 (−1306 to − 636)	1164 (594 to 1884)	−13652 (−16760 to −8166)	9692 (4944 to 15693)

dikes (*9*) (fig. S8). They also include drivers of gain such as mangrove planting, restoration activities, or coastal modifications to promote tidal exchange (Fig. 2B and fig. S8).

At the continental scale, Asia was identified as the global center of tidal wetland loss from direct human activities (fig. S9). In Asia, direct drivers accounted for more than two-thirds of the losses of each ecosystem (mangrove, 75%; tidal marsh, 69%; tidal flats; 62%; table S10), confirming the negative effects of widespread coastal transformation on coastal ecosystems. Although the impact of coastal development on mangroves and tidal wetlands have been previously reported (*9*, *14*), our results reveal that Asian tidal marshes have similarly been severely degraded by human activities. Compared with Asia, direct human activities had a much lesser role in the losses of tidal wetlands in Europe (28%), Africa (27%), North America (9%), South America (2%), and Oceania (0%; fig. S9).

Indirect or ex situ drivers include both natural coastal processes and those influenced by human activities remotely from the location of observed change. They include processes of isostatic change (*21*), sea level rise (*8*), storm impacts (*22*), erosion and progradation (*22*), along-shore coastal development (*9*), and the combined effects of all of the above. More than 90% of tidal wetland losses in North America (91%), South America (98%), and Oceania (100%) were attributed to indirect drivers (fig. S9). Globally, indirect drivers accounted for most losses of tidal marshes (78%) and tidal flats (66%), whereas mangrove losses were equally a result of direct and indirect drivers (50%; Table S9).

Most tidal wetland gains (86%) were the result of indirect drivers, highlighting the prominent role that broad-scale coastal processes have in controlling tidal wetland extent and facilitating natural regeneration. However, disentangling the specific processes underpinning tidal wetland change is challenging with analyses conducted at large spatial scales. In most cases direct drivers could be clearly identified, but many indirect drivers operate over large spatial and temporal scales and may originate tens to thousands of kilometers from an observed tidal wetland change. Change in ecosystem extent can also be the result of more than one indirect driver or of interactions between drivers. Our work therefore suggests a need for continued monitoring, experiments, and models that can account for these complexities to help characterize and predict global tidal wetland dynamics.

There is potential to use our analysis, which is designed to be periodically updated, to track larger-scale coastal ecosystem restoration activities. Although there has been a surge in coastal restoration efforts worldwide (*27*), many of these have been unsuccessful (*10*). Monitoring progress of restoration remotely, independently, and at broad scales could contribute to reporting on international conservation initiatives such as the UN Decade on Ecosystem Restoration, on targets associated with the Convention on Biological Diversity, and on mitigation commitments made under the UN Framework Convention on Climate Change (*27*). The driver analysis indicated that 14% of observed tidal wetland gains were attributable to direct human interventions (table S9). These activities were most apparent for tidal marshes and were typically the product of site scale restoration activities (Fig. 2B and fig. S8).

Our analysis enables the detection and characterization of dynamic transitions among intertidal ecosystem types globally. Transitions have been linked to a number of physical and climatic factors such as sea level rise, geomorphic changes, and variation in temperature and rainfall (*28*, *29*). We found that 1.9% of the world's tidal wetlands exhibited transitions among ecosystem types over the study

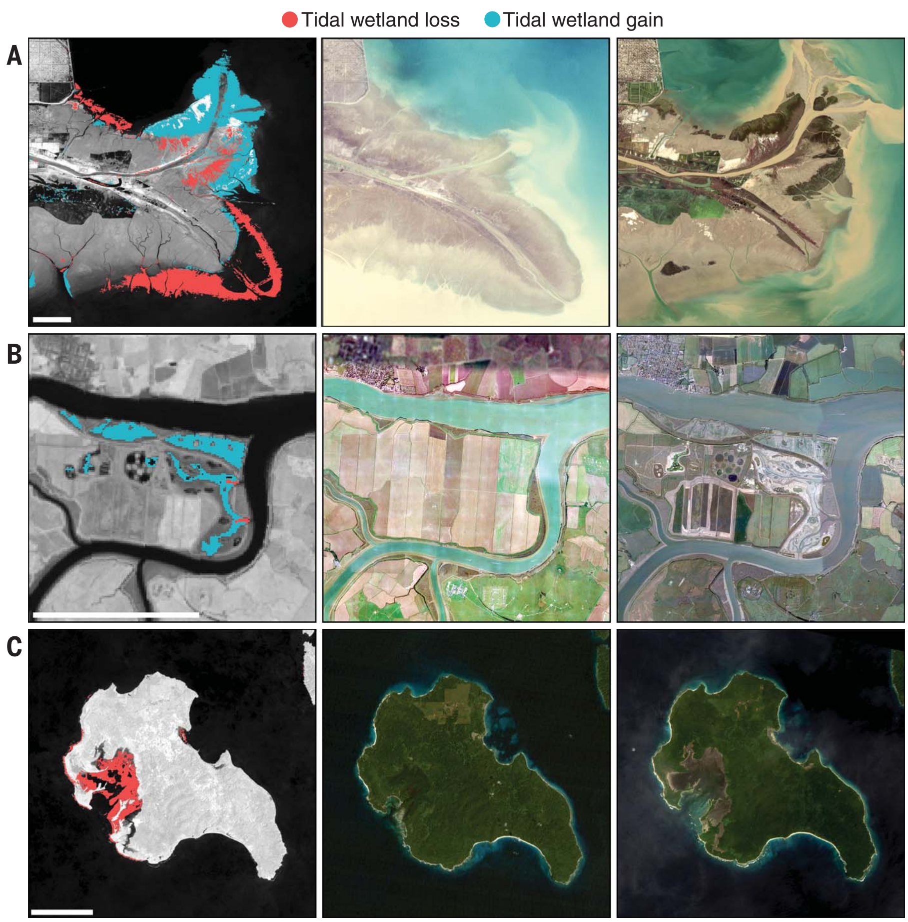

Fig. 2. Representative examples of 1999 to 2019 tidal wetland loss and gain. (**A**) Losses and gains of tidal flats and tidal marshes after diversion of the main channel in 1996 in the Yellow River delta in China (left). Reference images acquired in 1998 (middle) and 2020 (right). (**B**) Tidal marsh gain due to Europe's largest coastal wetland restoration project, UK (left). Reference images acquired in 1999 (middle) and 2018 (right). (**C**) Mangrove loss due to tectonic subsidence after the Aceh-Andaman earthquake of 2004, Katchal Island, Nicobar Islands (left). Reference images acquired 1992 (middle) and 2019 (right). Imagery data are from USGS (A) and (C) and Google Earth Pro (B). All scale bars are 5 km.

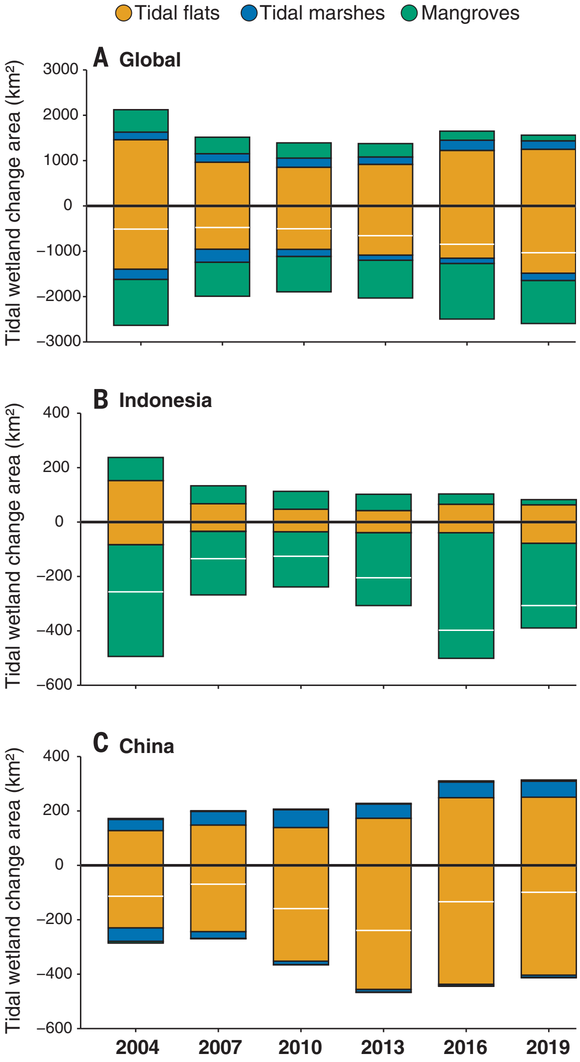

Fig. 3. Tidal wetland change totals from 1999 to 2019. Panels show the losses and gains of tidal wetlands per time step for (**A**) the global study area, (**B**) Indonesia, and (**C**) China. Shaded colors represent intertidal ecosystem types mapped by this analysis. White lines indicate the net change of tidal wetlands. Note that area change cannot be estimated for the initial time step of the analysis (1999 to 2001).

period (6700 km^2; table S4). Transition events tended to be spatially clustered with areas of large losses and gains and in many cases may be linked to the same drivers (*8*). More than 55% of transitions (>3600 km^2) involved colonization of tidal flats by marshes or mangroves and a further 27% consisted of transitions from mangrove to tidal marsh or vice versa (table S4).

Our classifier accurately detected known events of coastal change across the three ecosystem types. For example, the magnitude 9.2 Aceh-Andaman earthquake on 26 December 2004 caused up to 2.9 m of tectonic subsidence in the Andaman and Nicobar Islands, leading to land submergence and a loss of >90% of mangrove extent in some localities (Fig. 2C) (*30*). However, as for all earth observation-derived estimates of land cover change, there are limitations. These include the spatial resolution of sensor data (which limit the ability of our analysis to detect change in narrow linear features such as waterways), model uncertainty, errors of omission and commission, and a lack of polar coverage. Validation of our data products was effective in characterizing these uncertainties, which were propagated through our estimates of tidal wetland extent and change (tables S5 to S8).

By simultaneously mapping three of Earth's intertidal ecosystems, this work enables a synoptic view of change of three of the world's highly connected intertidal coastal ecosystems. This approach offers an advantage over single-ecosystem mapping studies as short- and long-term dynamic transitions between ecosystem types can cause considerable apparent change in individual ecosystems. Although our study is unable to account for the impact of centuries of anthropogenic coastal transformation and related pressures (*8*), it has established an observational record of recent tidal wetland changes with preliminary attribution of change drivers. Such information has the potential to promote objective monitoring of conservation and restoration efforts, assess the impacts of elevating pressures, guide new studies of changing ecosystem structure, function, and service provision in newly established tidal wetlands (*8*, *29*), and improve our understanding of the resilience of tidal wetlands in the face of global change. In turn, it can support efforts to anticipate the future of global coastal environments and to develop adaptive responses to change.

REFERENCES AND NOTES

1. E. B. Barbier *et al.*, *Ecol. Monogr.* **81**, 169–193 (2011).
2. M. D. Spalding *et al.*, *Conserv. Lett.* **7**, 293–301 (2014).
3. E. B. Barbier, *Science* **345**, 1250–1251 (2014).
4. D. A. Friess *et al.*, *Annu. Rev. Environ. Resour.* **44**, 89–115 (2019).
5. D. M. FitzGerald, Z. Hughes, *Annu. Rev. Earth Planet. Sci.* **47**, 481–517 (2019).
6. C. E. Lovelock *et al.*, *Nature* **526**, 559–563 (2015).
7. S. Fagherazzi *et al.*, *Rev. Geophys.* **50**, RG1002 (2012).
8. M. L. Kirwan, J. P. Megonigal, *Nature* **504**, 53–60 (2013).
9. N. J. Murray *et al.*, *Nature* **565**, 222–225 (2019).
10. E. Bayraktarov *et al.*, *Ecol. Appl.* **26**, 1055–1074 (2016).
11. M. L. Kirwan, S. Temmerman, E. E. Skeehan, G. R. Guntenspergen, S. Fagherazzi, *Nat. Clim. Chang.* **6**, 253–260 (2016).
12. M. Schuerch *et al.*, *Nature* **561**, 231–234 (2018).
13. P. Bunting *et al.*, *Remote Sens.* **10**, 1669 (2018).
14. L. Goldberg, D. Lagomasino, N. Thomas, T. Fatoyinbo, *Glob. Change Biol.* **26**, 5844–5855 (2020).
15. C. J. Mcowen *et al.*, *Biodivers. Data J.* **5**, e11764 (2017).
16. Materials and methods are available as supplementary materials.
17. P. I. Macreadie *et al.*, *Nat. Commun.* **10**, 3998 (2019).
18. M. Spalding, M. Leal, Eds., "The state of the world's mangroves 2021" (Global Mangrove Alliance, 2021).
19. J. H. Nienhuis *et al.*, *Nature* **577**, 514–518 (2020).
20. K. B. Gedan, B. R. Silliman, M. D. Bertness, *Annu. Rev. Mar. Sci.* **1**, 117–141 (2009).
21. J. P. M. Syvitski *et al.*, *Nat. Geosci.* **2**, 681–686 (2009).
22. D. Lagomasino *et al.*, *Nat. Commun.* **12**, 4003 (2021).
23. L. A. Deegan *et al.*, *Nature* **490**, 388–392 (2012).
24. X. Wang *et al.*, *Nat. Sustain.* **4**, 1076–1083 (2021).
25. M. Liu *et al.*, *Remote Sens.* **10**, 1933 (2018).
26. X.-P. Song *et al.*, *Nature* **560**, 639–643 (2018).
27. C. M. Duarte *et al.*, *Nature* **580**, 39–51 (2020).
28. K. C. Cavanaugh *et al.*, *Proc. Natl. Acad. Sci. U.S.A.* **116**, 21602–21608 (2019).
29. N. Saintilan *et al.*, *Science* **368**, 1118–1121 (2020).
30. P. Nehru, P. Balasubramanian, *For. Ecol. Manage.* **427**, 70–77 (2018).
31. N. Murray *et al.*, Code for high-resolution mapping of losses and gains of Earth's tidal wetlands, v1.0.0 Zenodo (2022); https://doi.org/10.5281/zenodo.5968865.
32. N. Murray *et al.*, Intertidal ecosystem training data for mapping Earth's tidal wetlands, Figshare (2022); https://doi.org/10.6084/m9.figshare.19121660.
33. N. Murray *et al.*, Data descriptor for Murray global tidal wetland change, v1.0.0 Zenodo (2022); https://doi.org/10.5281/zenodo.6503080.

ACKNOWLEDGMENTS

We thank R. Canto, M. Toor, and N. Y. Cárdenas for assistance with developing the training data. Landsat data are courtesy of NASA Goddard Space Flight Center and the US Geological Survey. We thank the Google Earth Engine team for providing Earth Engine, and M. Dewitt and N. Clinton for assistance with processing Landsat covariates in Earth Engine. **Funding:** This work was supported by the following: Australian Research Council Discovery Early Career Research Award DE190100101 (N.J.M.); Australian Research Council Discovery Australian Laureate Fellowship FL200100133 (C.E.L.); Julius Career Award from CSIRO (M.I.S.); Australian Research Council Linkage grant LP170101171 (V.H.). **Author contributions:** Conceptualization: N.J.M., T.A.W., and M.B.L. Data curation: N.J.M., P.B., R.L., and T.A.W. Methodology: N.J.M., T.A.W., M.B.L., C.E.L., V.H., and M.I.S. Formal Analysis: N.J.M., T.A.W., M.B.L., and S.D. Funding acquisition: N.J.M. Investigation – N.J.M., T.A.W., P.B., V.H., C.E.L., M.I.S., M.Sh., M.Sp., N.J.W., and M.B.L. Writing – original draft: N.J.M., T.A.W., and M.B.L. with input from all authors. Writing – review and editing: All authors. **Competing interests:** The authors declare that they have no competing interests. **Data and materials availability:** Code to

develop the global tidal wetland change product is available at Zenodo (*31*). Global tidal wetland training data is available at Figshare (*32*). The tidal wetland data products are viewable at www.globalintertidalchange.org and made available in several formats via Zenodo (*33*). Landsat Archive data are freely available courtesy of the U.S. Geological Survey (https://www.usgs.gov/landsat-missions/landsat-collection-1) and via Google Earth Engine Data Catalog (https://developers.google.com/earth-engine/datasets/catalog/landsat).

SUPPLEMENTARY MATERIALS

science.org/doi/10.1126/science.abm9583
Materials and Methods
Figs. S1 to S9
Tables S1 to S10
MDAR Reproducibility Checklist
References (*34*–*75*)

Submitted 26 October 2021; accepted 1 April 2022
10.1126/science.abm9583

Science

High-resolution mapping of losses and gains of Earth's tidal wetlands

Nicholas J. MurrayThomas A. WorthingtonPete BuntingStephanie DuceValerie HaggerCatherine E. LovelockRichard LucasMegan I. SaundersMarcus SheavesMark SpaldingNathan J. WalthamMitchell B. Lyons

Science, 376 (6594), • DOI: 10.1126/science.abm9583

Global shifts in tidal wetlands
Ecologically and economically important coastal wetlands are threatened by sea level rise and land use change. Murray *et al*. used high-resolution satellite imagery to assess the global extent of tidal wetlands and changes in wetland extent and distribution over the past two decades. They found that although over 13,000 square kilometers of tidal wetland have recently been lost, much of this decreasing extent has been offset by the creation of new wetlands. The greatest losses and gains were in tidal flats, but mangrove ecosystems showed the largest net decline in area globally. Direct human impacts on wetlands, including land transformation and restoration, are detectable from satellite imagery and account for 27% of wetland losses and gains. —BEL